Journal of Neural Engineering

PAPER

Reduce brain computer interface inefficiency by combining sensory motor rhythm and movement-related cortical potential features

To cite this article: Tengjun Liu *et al* 2020 *J. Neural Eng.* **17** 035003

IOP Publishing J. Neural Eng. 17 (2020) 035003 https://doi.org/10.1088/1741-2552/ab914d

Journal of Neural Engineering

CrossMark

RECEIVED
20 December 2019

REVISED
10 April 2020

ACCEPTED FOR PUBLICATION
7 May 2020

PUBLISHED
17 June 2020

PAPER

Reduce brain computer interface inefficiency by combining sensory motor rhythm and movement-related cortical potential features

Tengjun Liu[1,2,5], Gan Huang[1,2,6], Ning Jiang[3], Lin Yao[4] and Zhiguo Zhang[1,2,5]

1 School of Biomedical Engineering, Health Science Center, Shenzhen University, People's Republic of China
2 Guangdong Provincial Key Laboratory of Biomedical Measurements and Ultrasound Imaging, Shenzhen 518060, People's Republic of China
3 System Design Engineering Department, Center for Bioengineering and Biotechnology, University of Waterloo, Canada
4 School of Electrical and Computer Engineering, Cornell University, Ithaca, NY, United States of America

E-mail: huanggan1982@gmail.com

Keywords: BCI inefficiency, sensory motor rhythm, movement-related cortical potential, feature combination

Abstract

Objective. Brain Computer Interface (BCI) inefficiency indicates that there would be 10% to 50% of users are unable to operate Motor-Imagery-based BCI systems. Importantly, the almost all previous studieds on BCI inefficiency were based on tests of Sensory Motor Rhythm (SMR) feature. In this work, we assessed the occurrence of BCI inefficiency with SMR and Movement-Related Cortical Potential (MRCP) features. *Approach*. A pool of datasets of resting state and movements related EEG signals was recorded with 93 subjects during 2 sessions in separated days. Two methods, Common Spatial Pattern (CSP) and template matching, were used for SMR and MRCP feature extraction, and a winner-take-all strategy was applied to assess pattern recognition with posterior probabilities from Linear Discriminant Analysis to combine SMR and MRCP features. *Main results*. The results showed that the two types of features showed high complementarity, in line with their weak intercorrelation. In the subject group with poor accuracies (< 70%) by SMR feature in the two-class problem (right foot vs. right hand), the combination of SMR and MRCP features improved the averaged accuracy from 62% to 79%. Importantly, accuracies obtained by feature combination exceeded the inefficiency threshold. *Significance*. The feature combination of SMR and MRCP is not new in BCI decoding, but the large scale and repeatable study on BCI inefficiency assessment by using SMR and MRCP features is novel. MRCP feature provides the similar classification accuracies on the two subject groups with poor (< 70%) and good (> 90%) accuracies by SMR feature. These results suggest that the combination of SMR and MRCP features may be a practical approach to reduce BCI inefficiency. While, 'BCI inefficiency' might be more aptly called 'SMR inefficiency' after this study.

1. Introduction

Brain Computer Interfaces (BCI) technology provides direct communication pathways between the brain and an external device and thus may augment or restore human functions. However, 'BCI inefficiency' [1, 2], which occurs when a BCI system cannot discriminate brain patterns from all users, makes BCI less applicable in specific populations. Over the past two decades, the inefficiency problem in motor imagery (MI)-based BCI has aroused the attention of the academic research community. Guger *et al* [3] showed that 6.7% of the individuals showed accuracies lower than 60% in a study of a two-class BCI with 99 healthy subjects. Ang *et al* [4] showed that six out of 46 patients (13%) performed MI-based BCI of the stroke-affected hand at a chance level, with accuracies between 43% and 58%. However, the guidelines to specify the accuracy threshold to determine BCI inefficiency were not consistent across studies. It was further reported that the performance of MI-based BCI could be predicted by the resting state EEG and fMRI [5–7]. Overall, however, the

5 These authors contributed equally to this work.
6 Author to whom any correspondence should be addressed.

understanding about BCI inefficiency has remained insufficient.

The interrelatedness of a variety of underlying factors complicates the understanding of BCI inefficiency. First, the mode of motor imagery [8] and feedback [9] will affect the results of MI-based BCI directly. Second, transient factors, such as attention and fatigue [10, 11], make it impossible to predict whether a subject performing poorly in a certain experiment will also be unable to use the same BCI system in another setting. Third, training is a factor of key importance in MI-based BCI. The lack of skills needed to operate the system or an incomplete understanding of instructions given by the experimenters could also account for deficient performance [12, 13]. A case study by Pfurtscheller *et al* [14] showed that a 5 month training of a tetraplegic patient improved performance with an MI-based BCI from 65% to nearly 100%. Also, a 42-subject study with three sessions [15] showed a training effect on SMR topography. To obtain more robust results, a study design with the consistency actions from participants would be needed to minimize the interference of various factors in MI-based BCI.

Moreover, a crucial, but neglected issue, is that previous studies showing BCI inefficiency were based on the event-related desynchronization and synchronization (ERD/ERS) analysis of Sensory Motor Rhythm (SMR) [16]; whether other neurophysiological features during motor imagery tasks would be helpful to eliminate the BCI inefficiency remains unclear. Several methods, including adaptive autoregressive modeling [11, 14, 17], Common Spatial Pattern (CSP) procedures [18–20], and filter-bank type technique [21–23], have been developed for better SMR detection [24–26]. However, if the user cannot produce any discriminative SMR pattern, advanced algorithms for SMR detection cannot be applied [1]. Hence, improvements in SMR detection could reduce, but not eliminate, the issue of BCI inefficiency [1, 27, 28]. In fact, motor imagery produces not only SMR signals but also Movement-Related Cortical Potential (MRCP) signals [29]. MRCP is a slow negative brain potential with three components, the Bereitschafts-, motor-, and movement-monitoring potential, which are related to movement planning and execution [30]. For both real executed movement and motor imagery, SMR and MRCP occur simutaneously over the somatosensory area [16, 29–31]. SMR was considered be generated by the parameters changing in the nerual oscillations, and MRCP was viewed as a summation of long-lasting EPSPs at the apical dendrites [32]. Hence, with different underlineing neurophysiological mechanism, MRCP features would potentially provide independent complementary information to the SMR features for the BCI decoding. As reviewed by Shakeel *et al* [33], several signal-processing and classification methods have been used in MRCP detection, such as Independent Component Analysis [34], Locality Preserving Projection [35], and CSP [36]. The combination of of SMR and MRCP features is not new for the brain response decoding in the BCI appliocation. As early as in BCI competition III in 2005, MRCP has been used with SMR features together on the Dataset IVa of the MI-based BCI by the winner team [37]. But to the best of the authors' knowledge, none had addressed the BCI inefficiency problem with the combination of SMR and MRCP features.

In summary, the issue of BCI inefficiency relates to the fundamental question that whether all users can produce detectable brain activity. The contribution of a diversity of interacting factors complicates the understanding of BCI inefficiency. Additionally, most previous studies showing the inefficiency in MI-based BCI were restricted to the analysis of SMR features. In the present study, BCI inefficiency was investigated with a relatively simple experimental design, in which the combination of SMR and MRCP features was investigated in 93 subjects who were tested during two sessions on separate days.

2. Method

2.1. Experimental procedure

A total of 93 healthy participants (71 females, 22 males; 21.1 $\pm$ 5.3 years old) participated in the study for two sessions which were scheduled on different days separated by more than a week. The experimantal paradigm were the same for the two sessions. All participants were BCI-naïve individuals and had no known neurological deficits. All the participants gave their written informed consent before the experiment. Ethical approval of the study was sought and obtained from the Medical Ethics Committee, Health Science Center, Shenzhen University (No. 2 019 053).

The experimental paragdigm was illustrated in figure 1. During the experimental sessions, the participants were seated in comfortable chairs. They were instructed to perform three types of real executed in response to a visual cue displayed on a computer screen placed at a 1 meter distance. Cue presentation was programmed using Psychtoolbox-3 (http://psychtoolbox.org/) in Matlab. The participants were instructed to respond to the visual cue by gripping their left hand (LH) or right hand (RH), or to lift their right ankle (RF) for a duration of 3 s, i.e. until cue offset. No feedback was provided during the online recording. To ensure their motor areas being fully activated, the subjects were required to perform the real executed movements of LH, RF, and RH at a rate of twice per second or faster, at approximately 80% of their maximum voluntary contraction, while keeping their upper body still. There is no external tool, like metronome or hint on the screen, to remind the participant, since it may produce unnecessary evoked potential as an external stimulus. The experimenters continuously monitored whether the

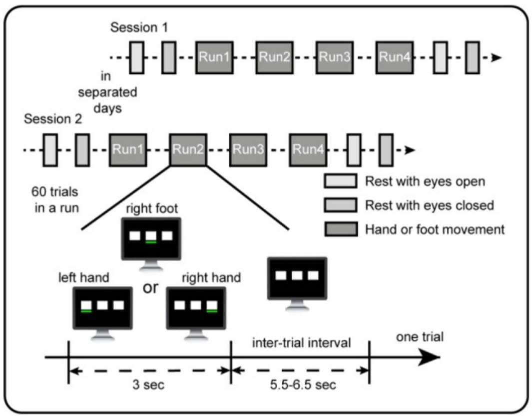

Figure 1. The experimental paradigm consists of two sessions in separated days. For each session, there were two runs of 1 minute resting state with eye open and closed, and four runs of movement. 60 trials of hand or foot movement was arranged randomly in each run. For each trial, the participant was required to perform right hand, left hand or right foot movement for 3 s, and the inter-trial interval lasts 5.5–5.6 s randomly.

movements from the participants met these standards, and corrected them when necessary. In this experiment, executed movement was used instead of motor imagery, and no feedback or training was given to the participants. The discussion about the pros and cons of the experiment design is arranged in section 4.

During both sessions, the participants were asked to have eight runs of EEG recording. The first and last two runs were 1 minuntes resting state with eye open and closed. A total of 240 movements (80 times for each movement type) were arranged in the middle four runs. The 240 trials were presented in random order arranged in four runs; the inter-trial interval was 5.5–6.5 s to make the participant unable to predict the coming event [38, 39]. Between the two adjacent runs, the participants could have a rest as they want.

2.2. Signal acquisition and pre-processing

EEG signals were obtained via a multichannel EEG electrode system (64 Channel, Easycap) and an EEG Amplifier (BrainAmp, Brain Products GmbH, Germany). The signals were recorded at a sampling rate of 1000 Hz by 64 electrodes, placed at the standard 10–20 positions, and referenced to the FCz channel. Before data acquisition, the contact impedance between EEG electrodes and cortex was calibrated to be lower than 20 kΩ, to ensure quality EEG signals during the experiments.

The raw EEG data were pre-processed by 0.01–200 Hz band-pass filtering and 50 Hz notch filtering; then, bad channel interpolation was performed and ICA was applied for artifact removal. After segmentation, EEG signals were re-referenced by Common Average Referencing [40]. To prevent overfitting in the classification [41], twenty-one channels surrounding C3, Cz, and C4 were selected for further analysis: F5, F3, F1, Fz, F2, F4, F6, C5, C3, C1, Cz, C2, C4, C6, P5, P3, P1, Pz, P2, P4, and P6.

Following common signal pre-processing, different types of processing were applied for SMR and MRCP signals. For SMR, only 8–30 Hz band-pass filtering was applied. For MRCP, EEG signals were filtered by 0.01–3 Hz band-pass filter, then down-sampled to 20 Hz, and corrected by subtracting the baseline from −1 to 0 s [40]. 4-order Butterworth zero-phase digital filter was applied for the bandpass filtering [42]. The bandwidth setting 8–30 Hz and 0.01–3 Hz corresponds to the main frequency bands for SMR and MRCP features. The 50 times down-sampling can retain the main information according to shannon's sampling theorem [43], but greatly improves the computational efficiency.

2.3. Feature extraction and classification

2.3.1. SMR features

The CSP method [20] was applied for SMR feature extraction as follows. First, for each trial, the normalized spatial covariance matrix is obtained by

$$\Sigma_i = \frac{X_i^T X_i}{trace\left(X_i^T X_i\right)},$$

in which $X_i \in R^{channel \times time}$ is the band-pass filtered EEG signals in the 0.5–3.5 s interval and the averaged spatial covariance matrix of $\Sigma^{(c)}$ was estimated from all of the training trials from different movement types ($c =$ LH, RF and RH). Next, by solving the generalized eigenvalue problems

$$\Sigma^{(c_1)}\omega = \lambda \Sigma^{(c_2)}\omega,$$

three pairs of spatial filters ω, corresponding to the largest and smallest eigenvalues λ of the spatial covariance matrix $\Sigma^{(c_1)}$ and $\Sigma^{(c_2)}$ from two different classes were obtained. As a final step, SMR features were extracted as the logarithmic band power coefficients of the spatially filtered signals. To address the three-class problem (LH vs. RH vs. RF), a one-versus-one strategy was applied for CSP-feature extraction. Hence, the feature size of SMR features was six for the two-class problem (LH vs. RH, LH vs. RF, and RH vs. RF) and 18 for the three-class problem.

2.3.2. MRCP features

A template-matching technique [44] was used for MRCP feature extraction. The template for each class,$TMPLT^{(c)}$,was obtained by averaging data from all the training trials from the 0–3 s interval within that class

$$TMPLT^{(c)} = \frac{1}{|I_c|}\Sigma_{i \in I_c} X_i,$$

Where I_c is the set of indices of the training trials corresponding to each class ($c =$ LH, RF and RH), $|I_c|$

is the size of set, and $X_i \in R^{channel \times time}$ is the EEG signal with 0.01–3 Hz band pass filtering, downsampling and baseline correction by the special pre-processing for MRCP. For both the training and testing trials, the MRCP features, $Fea\,(X_i, c)$, were extracted by calculating the dot product between the trial and three templates

$$Fea\,(X_i, c) = \left\langle X_i, TMPLT^{(c)} \right\rangle,$$

where $\langle \cdot, \cdot \rangle$ is the dot product along the dimension of time. Since 21 channels were used, the feature size of the MRCP features was 42 for the two-class problem and 63 for the three-class problem.

2.3.3. classification

Linear Discriminant Analysis (LDA) [45] was applied to classify SMR and MRCP features separately. Let $S = \Sigma_{i=1}^{2} \Sigma_{x \in D_i} (x - \mu_i)(x - \mu_i)^T$ to be the within-class scatter matrix, $\mu_i = \frac{1}{N_i} \Sigma_{x \in D_i} x$ to be the mean value of features in class i, the linear discrimination function would be

$$g(x) = \omega^T x + \omega_0,$$

where $\omega = S^{-1}(\mu_1 - \mu_2)$ and $\omega_0 = -\frac{1}{2}(\mu_1 + \mu_2)^T S^{-1} (\mu_1 - \mu_2)$. To account for the increased dimensionality, we did not combine the two types of features directly to train a new classifier. Instead, a winner-takes-all strategy was applied. Specifically, the label of each testing trial was predicted by the maximum posterior probabilities of the two LDA classifiers, which were trained separately for SMR and MRCP features. A trial-wise leave-one-out cross-validation [45, 46] was applied for within-subject level predictions.

2.4. Statistic analysis

2.4.1. The threshold for BCI inefficiency

The tested null hypothesis stated that one user could not produce any detectable brain activity for a given BCI system. Permutation tests were applied to generate the distribution for accuracy at chance level, which depended on the number of classes and trials in the task. Hence, in cases where the accuracy of the BCI system was established to lie within the 95% confidence interval of the distribution, we accepted the null hypothesis and considered the subject as BCI inefficient. The results from permutation tests are the same as those established by Müller-Putz's analysis [47]. When considering N datasets per test, the 95% confidence interval was adjusted to a (1–0.05/N) × 100% by Bonferroni correction. If the N datasets with the corresponding accuracies were all outside of the confidence interval, then statistically we rejected the null hypothesis and concluded that all users could produce detectable brain activity, and no inefficiency problem occurred in the examined BCI system.

The inefficiency threshold is related to the number of datasets and trials studies. For the two-class problem, the 95% confidence interval was 65.0% with 40 trials per dataset, which decreased to 57.5% with 160 trials per dataset. In the present study, 186 datasets (93 subjects; 2 sessions) were analyzed, with 160 trials for the two-class problem and 240 trials for the three-class problem. The boundaries for the 99.97% confidence interval with Bonferroni correction were circa 64.4% for the two-class problem and 44.6% for three-class problems. The observed proportion of datasets with accuracies below these thresholds represents the 'inefficiency rates' for the BCI system under study.

2.4.2. Correlaction analysis

To illustrate the effectiveness of feature combinations, Pearson's linear correlation coefficient was firstly performed between the classification accuracy with SMR and MRCP features separately in the two-class classification problem RF vs. RH.

Furthermore, since the performance with SMR features could be predicted by the resting state EEG [5], It would also be intersting to explore the suituation for MRCP features. Hence, the correlation analysis were also performed between resting state EEG and classification accuracy. Specifically, the logarithmic power spectral density (logPSD) was extracted from the resting state EEG signals with eyes closed by Welch's averaged modified periodogram with 2 s segmentation and 50% overlap. Pearson's correlation coefficient were estimated between logPSD and the classification accuracy with SMR and MRCP features separatly for each channel and each frequency bin.

3. Results

3.1. SMR and MRCP visualization

Most MI-based BCI systems rely on the fact that the amplitude of SMR can be controlled voluntarily by users. The time courses of SMR (8–30 Hz) by executed real movements of LH, RF, and RH are shown in the left panel in figure 2, with corresponding topographies from 0.5 to 3 s. During the movements, ERD produced by LH and RH were stronger than that generated by RF. For hand movements, contralateral electrodes displayed slightly larger ERD than the electrodes in the ipsilateral area. After termination of movements, ERS occurred on the corresponding sensorimotor area with an equal amplitude for all the three types of movements.

The time courses of the amplitude of MRCP for LH, RF, and RH are shown in the right panel in figure 2, together with the corresponding topographies between 0.5 and 3 s. The cue-based movement makes the Bereitschafts-potential component (ranging from 0 to 0.4 s) shorter than the self-paced one. Different from the transient movement, the three-second steady movement in this experiment increased the duration of the motor potential components. The amplitude of MRCP for RF was found to be more negative than those for LH and RH.

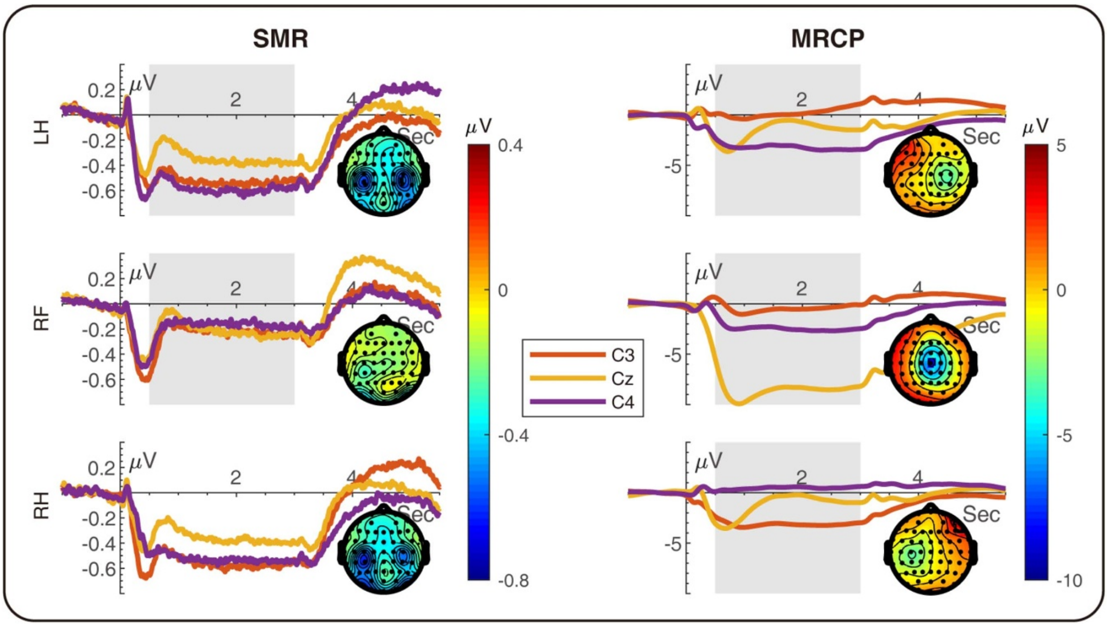

Figure 2. The grand averaged Sensory Motor Rhythm (SMR) and Movement Related Cortical Potential (MRCP) during the real movement of the left hand (LH), right foot (RF), and right hand (RH) from all subjects at channel C3 in red, Cz in yellow, and C4 in purple. The topographical maps were obtained by calculating the averaged amplitude at all channels in the shade time interval from 0.5 to 3 s after the cue turning on. In the left panel, the time courses of the SMR signals have been calculated by Hilbert transform after 8–30 Hz band-pass filtering. In the right panel, the time courses of the MRCP signals have been obtained by 0.01–3 Hz band-pass filtering. All results are based on the common average reference and base correction to −1 to 0 s.

Table 1. The performance of SMR and MRCP features used in the classification of RF vs. RH.

	Accuracies (%)			Correlation between Exp1 and Exp2	
Feature	Exp1	Exp2	Avg	r	p
SMR	80.57	75.99	78.28	0.86	6.91×10^{-28}
MRCP	81.10	77.19	79.14	0.75	4.06×10^{-18}
Both	88.90	84.72	86.81	0.81	1.01×10^{-22}

3.2. Classification results

3.2.1. Two-class classification

Take the two-class classification problem RF vs. RH for example. The mean classification accuracy was 78.3% ± 13.2% for SMR features among the 186 datasets; for MRCP features, an accuracy of 79.1% ± 8.2% was achieved. The combination of both two features improved the accuracy to 86.8% ± 8.3%. Further analysis showed high correlation coefficients (> 0.75) between the first and second sessions; they were statistically significant for all of the three types of features used in the classification. Compared with session 1, a decline of circa 4% for the classification accuracy in session 2 could be observed. All results are summarized in table 1.

By sorting the results from the 186 datasets in ascending order (figure 3(A)), the inefficiency rates were found to be 14.5% for SMR features (red curve), 4.3% for MRCP features (yellow curve), and 0% for the two features in combination (purple curve). Compared with SMR features, MRCP features were associated accuracies with lower variance across subjects. Combining SMR and MRCP features improved the accuracies, with all subjects' performance higher than the threshold.

Based on the results from SMR features, the 186 datasets could be divided into three groups, with poor (< 70%), moderate (70%–90%), and good (> 90%) results. The bar graph in figure 3(B) shows the performance of the three feature types in these three groups. In contrast to the stepwise growth for the performance of SMR feature (red bars), the results from MRCP feature were similar (yellow bars) in the three groups. Feature combination (purple bars) yielded better results than single features in all the three groups. For the poor-results group (< 70%), the mean accuracies increased from 62.2% by SMR feature to 79.5% when two features were combined. More importantly, the combination of two features increased the accuracies for all datasets in this group above the inefficiency threshold of 64.4%.

Detailed comparisons of the performance of these three types of features are shown in figures 3(C) and (D). The weak correlation coefficient ($r = 0.16$, $p = 0.03$ in figure 3(B)) proves the high complementarity between the two features. Hence, as shown in figure 3(D), feature combination improved the classification performance greatly in most datasets, especially in the datasets with lower accuracies for SMR features.

3.2.2. Three-class classification

For the classification of LH vs. RF vs. RH (figure 3(E)), the BCI inefficiency problem was less

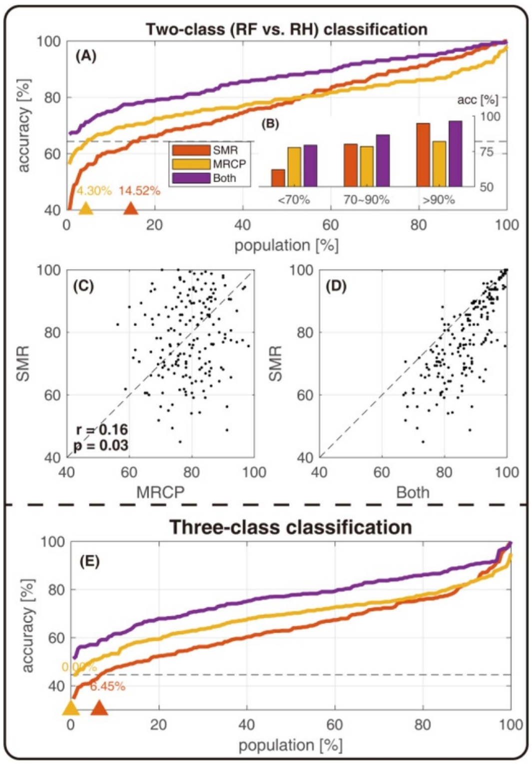

Figure 3. The classification results. For the two-class classification problem, (A) the sorted recognition accuracies from 186 datasets (93 subjects; 2 sessions) are shown by curves in different colors; SMR in red, MRCP in yellow, and both two features in purple. The dashed line indicates the inefficiency threshold of 64.4%. The triangles with different colors indicate the inefficiency rates. (B) The bar graph indicates the comparison of the classification accuracies with three types of features in three groups, which are poor (< 70%), moderate (70%–90%), and good (> 90%) by the results of SMR. (C) The pairwise comparison of the accuracies between SMR and MRCP features from 186 datasets. (D) The pairwise comparison of the accuracies between SMR and both features from 186 datasets. Similar results for three-class classification is shown in (E).

severe when three types of movements involved in the classification (inefficiency rates: 6.5% for SMR, 0.1% for MRCP, and 0% for both).

3.3. Neurophysiological predictor

As is shown in figure 4, both the classification results from SMR and MRCP features can be predicted by resting state EEG with eye closed.

For SMR features, the high correlation coefficient came from mu band (10–13 Hz) near channel C3 and C4. This result is consistent with that from Blankertz *et al* [5]. In addition, the second peak cames from beta band (20–23 Hz) with different topographies. Gamma band (except 50 Hz power frequency interference) also showed a negtive correlation results.

For MRCP features, the logPSD of the resting state EEG at mu (10–13 Hz) and beta (20–23 Hz) band was less correlated with the classification accuracies, in which the correlation coefficient were close to zeros at the the trough of the curve. By careful observation, it can be found that trough of the curve is a little

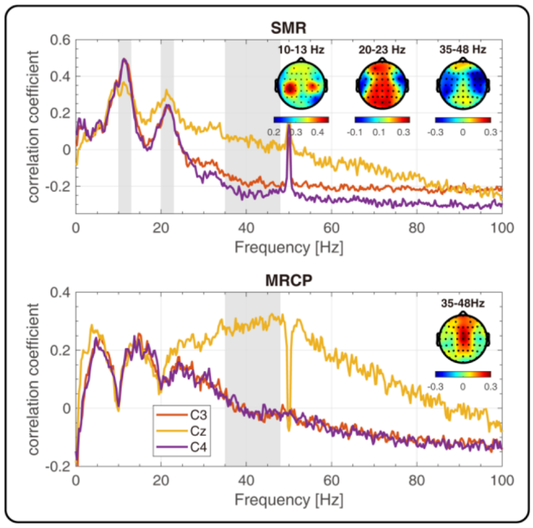

Figure 4. Correlation between logPSD from resting state EEG with eye closed and the classification accuracy with SMR and MRCP features separately at channel C3, Cz and C4. The scalp topographies illustrated the mean correlation coefficient in the corresponding brain rhythm 10–13 Hz, 20–23 Hz and 35–48 Hz.

earlier than the peak for SMR features. Furthermore, the gamma band spectrum at channel Cz showed a positive correlation results, especially the low gamma band (35–48 Hz).

Due to length limitations, only the correlation results with eye closed for SMR and MRCP features was presented in the manuscript. The correlation coefficient with eye open were similar with that was illustrated in figure 4, but slightly higher at 10–13 Hz for SMR features and slightly lower at 35–48 Hz for MRCP features.

4. Discussion

In the present study, the issue of BCI inefficiency was investigated by using both SMR and MRCP features. Considering that the interrelatedness of a variety of underlying factors complicates the understanding of BCI inefficiency, we tried to make the experimental design and methodology as simple as possible to help us understand this issue. The discussion of these factors are as follows,

4.1. The threshold for BCI inefficiency problem

BCI inefficiency indicates that a certain percentage of users perform with a ‘chance’ accuracy. However, there are no guidelines to determine the inefficiency threshold for accuracy. As noted by Allison *et al* [1], 6.7% of subjects showed accuracies of less than 60% in Guger’s study [3] and 48.7% subjects with accuracies less than 70%. Thus, fairly small changes in the definition of threshold can dramatically affect the percentage of the subjects’ scores classified as inefficient.

In the present study, permutation tests with Bonferroni correction were applied to determine the threshold, related to the number of datasets and trials in the studies. Bonferroni correction reduces the number of false positive results but is also very conservative, producing a higher rate of false negatives. Assuming there are 186 subjects with a true performance of 70% in a two-class problem, simulations with 160 trials in 186 datasets showed that the probability for scores of some users to be classified as inefficient is 100%. It should be noted that such thresholds can only be used to determine whether subjects achieve results at chance level but not to assess how well the subjects can use the BCI system.

In this study, 14.5% of datasets showed accuracies less than 64.4% in the classification of RH and RF by SMR features. Considering the different thresholds, this result is compatible with that found in Guger's study [3]. The inefficiency rate could be reduced to 0 by using both SMR and MRCP features in all the examined classification problems, except LH vs. RH. The three-class problems showed lower inefficiency rates than two-class problems, because chance level efficiency in three-class problems means that any two classes in the three classes cannot be distinguished.

4.2. Decoding algorithms

In this study, CSP and template matching methods were used for SMR- and MRCP-feature extraction, and LDA was applied for classification. CSP is the basic algorithm for decoding SMR features. Considering the poor spatial resolution, CSP algorithm could make full use of spatial correlation among channels to make the difference between the two classes maximum [20]. Hence, CSP achieved a better performance than directly using power band and logPSD fetures, and widely used in the ERD/ERS based SMR feature decoding [11, 14, 17]. Several methods, such as common spatio-spectral pattern [48], common sparse spectral spatial pattern [49] and filter bank CSP [21–23] are developped based on it. Since the motion detection by MRCP has becoming a research hotspot in the recent years, various methods has been proposed [34–36]. But there is no open competition, like BCI competition, to make an objectively evaluation on these methods. Templated matching technique was widely used for MRCP decoding [50, 51] because of its simplicity and effectiveness. In this study, the basic decoding algorithms, CSP and templated matching were applied because of their stable performance and the smaller number of hyperparameters to select, which should make the results in this paper easier to be compared with previous and future studies.

There is a clear need for further improvements by using the state-of-art and/or newly developed algorithms. The extent to which the new algorithm can improve the busyness of the brain-computer interface is also an important issue to consider. Future studies should explore the deep learning method in automatic feature extraction, to address the BCI-inefficiency issue.

4.3. Inefficiency prediction

SMR and MRCP are both motor related brain response, but are considered with different neurophysiological mechanisms [32]. In this study, two evidences, the weak correlation between SMR and MRCP performances, and the correlation coefficient close to zero between mu rhythm resting state EEG and the MRCP performance, have also indirectly proven the different origions of SMR and MRCP. The results of this study suggest that the previously well-defined concept of 'BCI inefficiency' for MI-based BCI might be more aptly called 'SMR inefficiency'. The inclusion of MRCP features greatly improved the performance in individuals with poor performance on SMR features. The previously SMR-based index for inefficiency predictions in Ref. [5] may not work well for the combination of SMR and MRCP features, it is necessary to develop the new prediction index in the future.

4.4. Comparison of executed movement and motor imagery

In this study, real executed movement, instead of motor imagery, was examined to explore the inefficiency problem in MI-based BCI, which is an important feature in experiment design but also the major limitation of this work.

By monitoring real movements, the experimenter can determine the completion of the participant's movement while minimizing the variance contributed by fatigue, attention, etc Since motor imagery tasks are new for BCI-naïve participants, different individuals might have a different understanding of the instructions. In addition, motor imagery is largely a mental process, which makes it difficult to monitor differences in participation in different subjects. Logically, all these factors might also increase the inefficiency in MI-based BCI. However, real executed movements are relatively simple tasks for which no training is needed. Participants can complete the task easily at a variety of levels of attention and fatigue. While it is not possible to ensure the consistency of mental states for different participants in experimental settings, their movements can be standardized to a certain degree. For this reason, the results demonstrated that BCI inefficiency cannot be attributed primarily to inconsistent actions of subjects.

However, the lack of direct evidence from motor imagery constitutes a major limitation of the present study. We conclude that the combination of SMR and MRCP features could provide the accuracies above chance level in real executed movements. Although we still have no direct evidence, the results from the executed movements suggest that the inefficiency problem in MI-based BCI may be addressed by feature combination. Previously, it was reported that motor imagery and executed movement can produce SMR [16] and MRCP [30, 33] activity in the sensorimotor areas in a highly similar way but that the brain activity accompanying executed movements showed better signal noise ratios and could be detected more easily [52]. In addition, executed movement-based BCI has also been widely used in the rehabilitation of stroke patients [53]. Applying our current feature-fusion approach from real-movement to MI tasks would merit future investigation.

4.5. Feedback and training

In the present study, no feedback or training was provided to the participants. Feedback is an import element in BCI systems, and different types of feedback can affect their performance greatly [12]. Several studies have demonstrated that training with appropriate feedback effectively improves BCI performance [14, 15]. However, to identify the contribution of various factors to the BCI inefficiency problem, the impact of feedback and training was excluded as much as possible in the design of the present study. However, a lack of feedback was associated with a decrease in user engagement across time, resulting in lower accuracies during the second, compared to the first experimental session, although both sessions consisted of the same actions.

There is also another practical reason for excluding feedback and training. Since the performances of SMR and MRCP features are compared in this study, any kind of feature or their combination used for immediate feedback and training would be improper for use in the comparison, because participants might learn to generate specific brain activity patterns to improve their performance during the experiment.

5. Conclusion

In the present study, the problem of BCI inefficiency was examined in an experiment featuring real executed movements without feedback or training, in 93 participants during two sessions that were scheduled on separate days. Performances based on only SMR or MRCP features were compared with those based on their combination.

Since executed real movements were used instead of motor imagery, the actions from all participants could be kept maximally consistent. Hence, we could confirm that the existence of BCI inefficiency on SMR features, which was also happened on MRCP features. However, the weak correlation between the two features suggested that MRCP features provide complementary information to SMR features. Combining two features is an effective way to improve the recognition rate in MI-based BCI systems. This improvement was particularly evident in participants with poor performance on SMR features. By using both features, all participants had their performance in the classification problem of RF vs. RH above chance level, a finding that turned out to be reproducible in the two-session experiment.

Acknowledgments

This work was supported by the National Natural Science Foundation of China (Nos. 61701316 and 81871443), the Science, Technology and Innovation Commission of Shenzhen Municipality Technology Fund (Nos. JCYJ20170818093322718 and JCYJ20190808173819182), and the Shenzhen Peacock Plan (No. KQTD2016053112051497).

ORCID iDs

Gan Huang https://orcid.org/0000-0001-9895-6163
Ning Jiang https://orcid.org/0000-0003-1579-3114

References

[1] Allison B Z and Neuper C 2010 *Could Anyone Use a BCI?* (London: Springer) pp 35–54
[2] Edlinger G, Allison B Z and Guger C 2015 *How Many People Can Use a BCI System? Clinical Systems Neuroscience* (Tokyo: Springer) pp 33–66
[3] Guger C, Edlinger G, Harkam W, Niedermayer I and Pfurtscheller G 2003 How many people are able to operate an EEG-based brain-computer interface (BCI)? *IEEE Trans. Neural Syst. Rehabil. Eng.* **11** 145–7
[4] Ang K K, Guan C, Chua K S G, Ang B T, Kuah C W K, Wang C, Phua K S, Chin Z Y and Zhang H 2011 A large clinical study on the ability of stroke patients to use an EEG-based motor imagery brain-computer interface *Clin. EEG Neurosci.* **42** 253–8
[5] Blankertz B, Sannelli C, Halder S, Hammer E M, Kübler A, Müller K-R, Curio G and Dickhaus T 2010 Neurophysiological predictor of SMR-based BCI performance *Neuroimage* **51** 1303–9
[6] Zhang T, Liu T, Li F, Li M, Liu D, Zhang R, He H, Li P, Gong J and Luo C 2016 Structural and functional correlates of motor imagery BCI performance: insights from the patterns of fronto-parietal attention network *Neuroimage* **134** 475–85
[7] Zhang R, Yao D, Valdés-Sosa P A, Li F, Li P, Zhang T, Ma T, Li Y and Xu P 2015 Efficient resting-state EEG network facilitates motor imagery performance *J. Neural Eng.* **12** 66024
[8] Neuper C, Scherer R, Reiner M and Pfurtscheller G 2005 Imagery of motor actions: differential effects of kinesthetic and visual–motor mode of imagery in single-trial EEG *Cogn. Brain Res.* **25** 668–77
[9] Ono T, Kimura A and Ushiba J 2013 Daily training with realistic visual feedback improves reproducibility of event-related desynchronisation following hand motor imagery *Clin. Neurophysiol.* **124** 1779–86
[10] Myrden A and Chau T 2015 Effects of user mental state on EEG-BCI performance *Frontiers Hum. Neurosci.* **9** 308
[11] Schlögl A, Lugger K and Pfurtscheller G 1997 Using adaptive autoregressive parameters for a brain-computer-interface experiment *Proc. of the 19th Annual Int. Conf. of the IEEE Eng. Med. Biol. Soc.'Magnificent and Emerging Opportunities in Medical Engineering'(Cat. No. 97CH36136)* vol 4 pp 1533–5

[12] Thompson M C 2019 Critiquing the concept of BCI illiteracy *Sci. Eng. Ethics* **25** 1217–33
[13] Li J and Zhang L 2012 Active training paradigm for motor imagery BCI *Exp. Brain Res.* **219** 245–54
[14] Pfurtscheller G, Guger C, Müller G, Krausz G and Neuper C 2000 Brain oscillations control hand orthosis in a tetraplegic *Neurosci. Lett.* **292** 211–4
[15] Meng J and He B 2019 Exploring training effect in 42 human subjects using a non-invasive sensorimotor rhythm based online BCI *Frontiers Hum. Neurosci.* **13** 128
[16] Pfurtscheller G and Neuper C 2001 Motor imagery and direct brain-computer communication *Proc. IEEE* **89** 1123–34
[17] Pfurtscheller G, Neuper C, Guger C, Harkam W, Ramoser H, Schlogl A, Obermaier B and Pregenzer M 2000 Current trends in Graz brain-computer interface (BCI) research *IEEE Trans. Rehabil. Eng.* **8** 216–9
[18] Koles Z J 1991 The quantitative extraction and topographic mapping of the abnormal components in the clinical EEG *Electroencephalogr. Clin. Neurophysiol.* **79** 440–7
[19] Fukunaga K 2013 *Introduction to Statistical Pattern Recognition* (Amsterdam: Elsevier)
[20] Blankertz B, Tomioka R, Lemm S, Kawanabe M and Muller K-R 2008 Optimizing spatial filters for robust EEG single-trial analysis *IEEE Signal Process. Magn.* **25** 41–56
[21] Ang K K, Chin Z Y, Zhang H and Guan C 2008 Filter bank common spatial pattern (FBCSP) in brain-computer interface *2008 IEEE Int. Joint Conf. on Neural Networks* pp 2390–7
[22] Higashi H and Tanaka T 2013 Simultaneous design of FIR filter banks and spatial patterns for EEG signal classification *IEEE Trans. Biomed. Eng.* **60** 1100–10
[23] Thomas K P, Guan C, Lau C T, Vinod A P and Ang K K 2009 A new discriminative common spatial pattern method for motor imagery brain–computer interfaces *IEEE Trans. Biomed. Eng.* **56** 2730–3
[24] Pfurtscheller G and Aranibar A 1979 Evaluation of event-related desynchronization (ERD) preceding and following voluntary self-paced movement *Electroencephalogr. Clin. Neurophysiol.* **46** 138–46
[25] Pfurtscheller G and Da Silva F H L 1999 Event-related EEG/MEG synchronization and desynchronization: basic principles *Clin. Neurophysiol.* **110** 1842–57
[26] Padfield N, Zabalza J, Zhao H, Masero V and Ren J 2019 EEG-based brain-computer interfaces using motor-imagery: techniques and challenges *Sensors* **19** 1423
[27] Blankertz B, Losch F, Krauledat M, Dornhege G, Curio G and Müller K-R 2008 The Berlin brain-computer interface: accurate performance from first-session in BCI-naive subjects *IEEE Trans. Biomed. Eng.* **55** 2452–62
[28] Brunner C, Allison B Z, Krusienski D J, Kaiser V, Müller-Putz G R, Pfurtscheller G and Neuper C 2010 Improved signal processing approaches in an offline simulation of a hybrid brain–computer interface *J. Neurosci. Methods* **188** 165–73
[29] Hallett M 1994 Movement-related cortical potentials *Electromyogr. Clin. Neurophysiol.* **34** 5–13
[30] Shibasaki H and Hallett M 2006 What is the Bereitschaftspotential? *Clin. Neurophysiol.* **117** 2341–56
[31] Balconi E 2009 The multicomponential nature of movement-related cortical potentials: functional generators and psychological factors *Neuropsychol. Trends* **5** 59–84
[32] Pfurtscheller G and Neuper C 1997 Motor imagery activates primary sensorimotor area in humans *Neurosci. Lett.* **239** 65–68
[33] Shakeel A, Navid M S, Anwar M N, Mazhar S, Jochumsen M and Niazi I K 2015 A review of techniques for detection of movement intention using movement-related cortical potentials *Comput. Math. Methods Med.* **2015**
[34] Jiang N, Gizzi L, Mrachacz-Kersting N, Dremstrup K and Farina D 2015 A brain–computer interface for single-trial detection of gait initiation from movement related cortical potentials *Clin. Neurophysiol.* **126** 154–9
[35] Xu R, Jiang N, Lin C, Mrachacz-Kersting N, Dremstrup K and Farina D 2013 Enhanced low-latency detection of motor intention from EEG for closed-loop brain-computer interface applications *IEEE Trans. Biomed. Eng.* **61** 288–96
[36] Yao L, Chen M L, Sheng X, Mrachacz-Kersting N, Zhu X, Farina D and Jiang N 2017 Common spatial pattern with polarity check for reducing delay latency in detection of MRCP based BCI system *2017 8th Int. IEEE/EMBS Conf. on Neural Engineering* pp 544–7
[37] Wang Y, Gao S and Gao X 2006 Common spatial pattern method for channel selelction in motor imagery based brain-computer interface *2005 IEEE Eng. Med. Biol. 27th Annual Conf.* pp 5392–5
[38] Liberati G, Algoet M, Klöcker A, Santos S F, Ribeiro-Vaz J G, Raftopoulos C and Mouraux A 2018 Habituation of phase-locked local field potentials and gamma-band oscillations recorded from the human insula *Sci. Rep.* **8** 1–13
[39] Mancini F, Pepe A, Bernacchia A, Di Stefano G, Mouraux A and Iannetti G D 2018 Characterizing the short-term habituation of event-related evoked potentials *ENeuro* **5**
[40] Hu L and Zhang Z 2019 *EEG Signal Processing and Feature Extraction* (Berlin: Springer)
[41] Huang G, Liu G, Meng J, Zhang D and Zhu X 2010 Model based generalization analysis of common spatial pattern in brain computer interfaces *Cogn. Neurodyn.* **4** 217–23
[42] Gustafsson F 1996 Determining the initial states in forward-backward filtering *IEEE Trans. Signal Process.* **44** 988–92
[43] Marks R J I I 2012 *Introduction to Shannon Sampling and Interpolation Theory* (New York: Springer)
[44] Jonas P, Major G and Sakmann B 1993 Quantal components of unitary EPSCs at the mossy fibre synapse on CA3 pyramidal cells of rat hippocampus *J. Physiol.* **472** 615–63
[45] Duda R O, Hart P E and Stork D G 2012 *Pattern Classification* (New York: Wiley)
[46] Wong T-T 2015 Performance evaluation of classification algorithms by k-fold and leave-one-out cross validation *Pattern Recognit.* **48** 2839–46
[47] Müller-Putz G, Scherer R, Brunner C, Leeb R and Pfurtscheller G 2008 Better than random: a closer look on BCI results *Int. J. Bioelectromagn.* **10** 52–55
[48] Lemm S, Blankertz B, Curio G and Muller K-R 2005 Spatio-spectral filters for improving the classification of single trial EEG *IEEE Trans. Biomed. Eng.* **52** 1541–8
[49] Dornhege G, Blankertz B, Krauledat M, Losch F, Curio G and Müller K-R 2006 Optimizing spatio-temporal filters for improving brain-computer interfacing *Adv. Neural Inf. Process. Syst.* pp 315–22
[50] Li S, Zhu Y, Huang G, Zhang L, Zhang Z and Huang K 2018 Detection of movement-related cortical potentials associated with emergency and non-emergency tasks *2018 IEEE 23rd Int. Conf. on Digital Signal Processing* pp 1–5
[51] Niazi I K, Jiang N, Jochumsen M, Nielsen J F, Dremstrup K and Farina D 2013 Detection of movement-related cortical potentials based on subject-independent training *Med. Biol. Eng. Comput.* **51** 507–12
[52] Morash V, Bai O, Furlani S, Lin P and Hallett M 2008 Classifying EEG signals preceding right hand, left hand, tongue, and right foot movements and motor imageries *Clin. Neurophysiol.* **119** 2570–8
[53] Silvoni S, Ramos-Murguialday A, Cavinato M, Volpato C, Cisotto G, Turolla A, Piccione F and Birbaumer N 2011 Brain-computer interface in stroke: a review of progress *Clin. EEG Neurosci.* **42** 245–52